Nanoscale

Plasma-assisted Destruction of Polystyrene Nanoplastics

Journal:	*Nanoscale*
Manuscript ID	NR-ART-06-2024-002498.R1
Article Type:	Paper
Date Submitted by the Author:	14-Nov-2024
Complete List of Authors:	Winburn, Matthew; University of Nebraska-Lincoln, Department of Chemistry Alvarado, Maria; North Central College, Chemistry Cheung, Chin Li; University of Nebraska-Lincoln, Chemistry

SCHOLARONE™
Manuscripts

Please do not adjust margins

ARTICLE

Plasma-assisted Destruction of Polystyrene Nanoplastics

Matthew R. Winburn,[a] Maria F. Alvarado,[b] and Chin Li Cheung*,[a]

Received 00th January 20xx,
Accepted 00th January 20xx

DOI: 10.1039/x0xx00000x

This study addresses the critical need for the effective removal of nanoplastics (1 nm to 1000 nm), which pose a significant environmental challenge due to their ease of entry into biological systems and poorly understood health impacts. We report our investigation of a plasma-assisted methodology with a falling film plasma reactor to destroy and remove 200-nm polystyrene nanoplastic particles from their aqueous solution. Using the nanoparticle tracking analysis, size exclusion chromatography, and total organic carbon (TOC) analysis, we examined the degradation kinetics of the nanoplastics upon plasma-assisted treatment. A nanoplastic removal rate of 98.4% by particle count was achieved in one hour of treatment. This rate increased to 99.3% after three hours of treatment, along with a 27.4% reduction in the TOC of the solution. The chromatography results indicate that the observed elimination of nanoplastic contaminants was likely through the production of short polystyrene oligomers with molecular weights roughly equivalent to those of two styrene units. The superior efficacy of the plasma-assisted methodology over traditional ozonation to destroy nanoplastics was also illustrated. Our results not only elucidate a hypothesized polystyrene radical decay mechanism but also demonstrate a potential and complementary approach for mitigating nanoplastic pollution in water purification strategies.

1. Introduction

Plastic production has increased dramatically in recent decades, with an estimated 12,000 million tons in landfills and the environment by 2050.[1] Despite its utility, the persistent nature of plastics presents significant challenges. Their degradation half-lives range from decades to over a millennium.[2] Microplastics (plastic particles of sizes in the range of 0.001 mm to 5 mm) have been in the public eye for several decades and are a pervasive pollutant. Nanoplastics (plastic particles of sizes ranging from 1 to 1000 nm) are a significantly more recent discovery and present unique challenges in environmental management and degradation technologies. Owing to their small sizes, these particles exhibit distinct physical and chemical behaviors which include increased mobility in ecosystems and a higher likelihood of penetrating biological barriers when compared to larger plastic debris.[3-5] This makes them particularly insidious pollutants because they can be transported across different environmental matrices and potentially accumulate in the food chain. Particularly, the persistence and ubiquity of polystyrene nanoplastics are compounded by their chemical stability and resistance to biodegradation which arise from their high molecular weight and the strength of the carbon-carbon bonds in the polystyrene polymer. The ubiquitous nature of the plastic particles has led to the emergence of the "plastisphere", a novel microbial habitat on microplastics and nanoplastics that facilitates their dispersal into ecosystems.[6] The potential toxicity of these particles in humans such as their ability to obstruct pulmonary structures or cross the blood-brain barrier underscores the imperative to develop effective solutions for their removal from waste and drinking water sources.[7-9] Current research on nanoplastics frequently highlights the significant gaps in our understanding of their environmental behaviors and impacts, making it imperative to develop efficient and scalable technologies for their removal or degradation. This backdrop of environmental and health challenges underscores the need for a broad spectrum of effective treatment methods. This study addresses this critical need by exploring the potential of the plasma-assisted destruction methodology which could provide a feasible solution for mitigating the environmental risks associated with these materials.

Conventional wastewater treatment methods, including flocculation and filtration, are commonly used to remove pollutants due to their simplicity and effectiveness.[10] In the USA, public water systems like those in Lincoln, Nebraska, integrate these techniques with advanced oxidation processes such as ozonation to enhance disinfection and facilitate the filtration of metals like manganese and iron.[11] However, these traditional techniques can lead to the contamination of filtration media with plastic particles, requiring careful disposal to avoid their environmental re-entry. In response to increasing microplastic and nanoplastic pollution, innovative approaches are being explored. For example, magnetic particle absorption has been illustrated to effectively remove nanoplastics, though it is less effective for larger particles.[12] Solar-powered nanorobotic sweeping can eliminate up to 96% of nanoplastics, significantly outperforming traditional methods that achieve less than 30% efficiency.[13, 14] Nonetheless, this method faces

[a] Department of Chemistry, University of Nebraska-Lincoln, Lincoln, Nebraska, USA. Email: ccheung2@unl.edu
[b] Department of Chemistry, North Central College, Naperville, Illinois, USA.
† Electronic Supplementary Information available: Plots of particle intensity versus size for plasma-treated sample solutions and electrical signals from an operating plasma reactor. See DOI: 10.1039/x0xx00000x

Please do not adjust margins

challenges in saline or low-light conditions, and it may risk environmental accumulation. Electrochemical oxidation treatments are also promising, and they have been demonstrated to achieve up to 86.8% pollutant removal in just 0.67 hours. Even so, they are limited by high electricity costs and the need for expensive precious metal electrodes.[15]

In contrast, plasma-assisted destruction (PAD) has emerged as a compelling alternative to traditional electrochemical and electrooxidation methods for water decontamination.[16-18] Plasma, the fourth state of matter, consists of electrons, ions, radicals, and excited molecules. It is classified into thermal and non-thermal types which is based on the temperature equilibrium between electrons and the chemical species in plasma.[19] While thermal plasma is composed of both electrons and chemical species at similar temperatures of 1000s K, non-thermal plasma possesses chemical species that are significantly cooler, making it ideal for sensitive applications like water treatment.[20, 21] Non-thermal plasma is typically generated in various reactor configurations which include common setups like point-to-plate and dielectric barrier discharge across a falling water film.[22] The efficacy of this technology in addressing waterborne organic contaminants such as insecticides is primarily due to its high oxidation potential driven by hydroxyl radicals.[23] These radicals are produced from water vapor in the air when plasma interacts with the air-water interface and directly in the water through the decay of shorter-lived radical species.[24]

Currently, advances in PAD treatment of plastics focus mostly on direct degradation and upcycling of solid plastics into chemical products. Although thermal plasma gasification processes can degrade mixed plastics into syngas, pyrolysis oil, and slag, they require high capital investment and energy consumption.[25] Recent developments in non-thermal PAD demonstrate its potential to degrade polyethylene, producing hydrogen and light hydrocarbons through hydrogenolysis.[26, 27] Radhakrishnan *et al.* showed that the non-thermal PAD process when combined with additional carbon dioxide and oxygen can upcycle polyethylene into syngas and valuable oleochemicals with high yields.[28] However, these thermal and non-thermal plasma approaches typically yield a broad variety of chemical products with low selectivity and require high starting temperatures, making them unsuitable for the direct treatment of plastic contaminants in water.

Herein we report our investigation and evaluation of the efficacy of a falling-film plasma reactor (FFPR) for destroying polystyrene nanoplastics (PS-NPs) in water and its potential for removing nanoplastics. Our study utilized the atmospheric plasma generated within an FFPR to treat aqueous solutions of 200-nm polystyrene nanospheres circulated over the surface of the reactor electrode. The FFPR was selected for its efficiency in oxidative processes and robustness against external variables such as salinity.[29, 30] This system is designed to maximize the contact area between the plasma and the aqueous solution, thereby increasing the generation and efficacy of reactive species such as hydroxyl radicals that are essential for the breakdown of polystyrene chains in our proof-of-principle study. Polystyrene nanospheres were chosen as a model system for polystyrene nanoplastics due to the pervasive use of polystyrene and distinct challenges. The results of this plasma-assisted treatment were compared to those of ozone degradation treatments of equivalent samples for simulating local municipal treatment processes. Based on the observed degradation products and kinetics, we proposed a mechanism for the cyclic degradation of polystyrene using hydroxyl radicals generated in plasma, akin to mechanisms observed in UV degradation processes. Post-treatment concentrations and sizes of the plastic particles were quantified using nanoparticle tracking analysis (NTA) with size-exclusion liquid chromatography (SEC) to provide additional validation. The total organic carbon analysis (TOC) was performed to assess the mineralization of the polymer following plasma-assisted treatment. The energy consumption of the current FFPR design was also assessed to offer insights into its power efficiency and operational costs. Finally, the benefits and limitations of this plasma-assisted destruction methodology were discussed for advancing water treatment technologies in combating persistent nanoplastic pollutants.

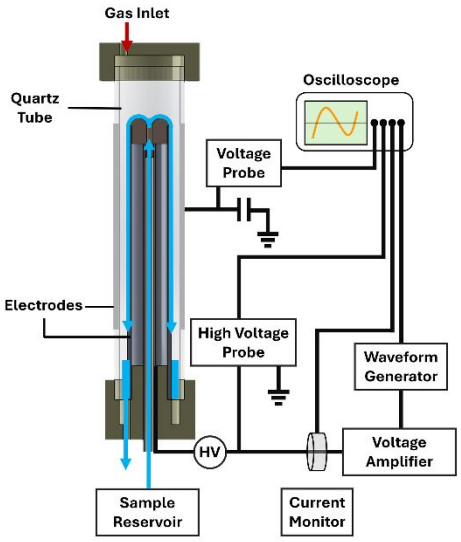

Fig 1. Schematic of a home-built falling-film plasma reactor used in this study. The blue arrows indicate the flow direction of solutions during the operation of the reactor.

2. Experimental

2.1 Materials

Polystyrene nanospheres with a nominal diameter of 200 nm (Lot 9936) were procured from Bangs Laboratories, Inc. (Fishers, IN, USA), featuring a manufacturer-listed effective diameter of 208.8 nm. Nanopure water with a resistivity of 18 MΩ•cm was sourced from a Synergy® system (VWR, Radnor, PA, USA), which purified deionized water for the preparation of aqueous nanosphere solutions.

2.2 Falling-Film Plasma Reactor (FFPR)

For this study, a home-built, 3D-printed dielectric barrier discharge falling-film plasma reactor (FFPR) was employed (Figure 1). The reactor setup comprised a reactor with a 250-mL

This journal is © The Royal Society of Chemistry 2024

glass reservoir beaker positioned underneath the reactor stand. The pen-size reactor's plasma chamber consisted of a quartz tube with an inner diameter (ID) of 13 mm and an outer diameter (OD) of 15 mm. This tube enclosed an inner electrode made from 304 stainless steel with dimensions of 8 mm ID × 10 mm OD and a length of 70 mm. The outer electrode was a 50 mm aluminum tape that was wrapped around the quartz tube and grounded through a 100 nF capacitor box. Air was allowed to flow freely into the reactor chamber through the top hole of the reactor cap to facilitate the generation of atmospheric plasma. A peristaltic pump facilitated the circulation of the nanoplastic solution from the reservoir through tubing that extended from the bottom of the reactor to the inner electrode at a flow rate of 30 mL/min. Exiting the fountain nozzle at the electrode's top, the solution formed a falling film along the outer surface of the inner electrode, driven by gravity and surface tension, before returning to the reservoir by gravity through additional tubing. The directional flow of the solution is depicted by arrows in Figure 1. A sinusoidal voltage of 10 kV peak-to-peak was applied to the reactor, generated by routing a signal from an AFG31012 Arbitrary Function Generator (Tektronix, Inc., Beaverton, OR, USA) through a Trek 10/40A-HS high-voltage amplifier (Advanced Energy, Eden Prairie, MN, USA). Voltage and current were monitored using a Cal Test Ct4028 high-voltage probe and a Pearson Model 150 current monitor, respectively. The electrical discharge was assessed by measuring the voltage drop across a 100 nF capacitor, with all associated waveforms recorded using a 4-channel oscilloscope (Rhode & Schwarz, U.S.A., Inc., Columbia, MD, USA).

2.3 Plasma-assisted degradation treatment of polystyrene nanoplastic solutions

The primary objective of this study was to evaluate the effectiveness of the plasma-assisted treatment on an aqueous solution of 200-nm polystyrene nanospheres as simulants for environmental nanoplastics. The initial concentrations of the solutions were approximately 0.001 wt.% of polystyrene nanospheres or 1.22×10^{10} particles per milliliter. For each experimental trial, 50 mL of the aqueous sample was introduced into the reactor beaker and circulated through the reactor at a rate of approximately 30 mL/min. The reactor was activated using an arbitrary function generator that applied a sinusoidal signal of 10 V peak-to-peak voltage at 10 kHz which was then amplified to 10 kV. The plasma was generated under ambient conditions and maintained for 180 minutes. Samples were collected at regular intervals for subsequent analysis.

2.4 Ozone-assisted degradation treatment of polystyrene nanoplastic solutions

To determine the effects of ozonation on the degradation of 200-nm polystyrene nanospheres in a simulated ozone treatment for potable water, a stream of ozone was bubbled into 50 mL of an aqueous solution of polystyrene nanospheres with a concentration of approximately 0.001 wt.% for 180 minutes. The sample was stirred constantly to emulate the mixing that occurred during the plasma treatment. The ozone was generated at a rate of 0.5-0.6 g/h by flowing 200 SCCM of oxygen (purity of 99.6%, Matheson Tri-Gas, Lincoln, NE, USA) through an MP-3000 ozone generator (A2Z Ozone Inc, Louisville, KE, USA). Samples of treated solutions were taken periodically for particle density analysis using the NTA method.

2.5 Sample characterization

The particle size distribution and particle count of the nanoplastic solutions were measured by NTA using a Malvern NanoSight NS300 (Malvern Panalytical, Malvern, UK). The particle counts were later verified using a ZetaView Mono (ParticleMetrix, Amersee, Germany). The molecular weights and relative concentrations of polymers in the samples were measured using an Agilent 1260 size-exclusion chromatograph (Agilent Technologies, Inc., Santa Clara, CA, USA) equipped with a refractive index/UV-Vis detector and an Agilent PLGel Mixed-D column. To determine the degree of mineralization, we tested the samples using a GE Sievers 900 Laboratory TOC Analyzer (GE Analytical Instruments, Boulder, CO) with the DataPro 900 software system, following our SOP (QC-3026) that aligns with the European Pharmacopeia (EP 2.2.44) and United States Pharmacopeia (<643>) methodologies for Total Organic Carbon Analysis. A 1-ppm carbon standard, prepared from a 1000-ppm standard using in-house water for injection (WFI), was employed for calibration.

3. Results

3.1 Effect of the plasma treatment on PS-NPs

Our investigation of the plasma-assisted methodology focused on determining the effect of the plasma-assisted destruction (PAD) treatment using an FFPR system on 200-nm polystyrene nanospheres (Figure 2a) in an aqueous solution of 0.001 wt.% nanoplastics. Polystyrene nanospheres were employed as model nanoplastic particles due to their nearly perfect spherical shape, contrasting with the often-irregular surface of environmental nanoplastics, thus facilitating a more accurate measurement of particle size and concentration (or particle count per milliliter). The selected concentration of the nanoplastic simulant approximates the upper limit observed in environmental contexts.[26, 31] The nanoparticle tracking analysis (NTA) technique was utilized in our study to provide insights into particle size and concentration by determining particles based on their average hydrodynamic diameters. The detection limits of this technique were confined to reliably identifying polymer fragments of no smaller than 10 nanometers and a limit of quantification of *ca.* 1×10^{7} particles per milliliter. This limitation highlighted the essential role of size exclusion chromatography (SEC) in complementing the particle size characterization, particularly for smaller fragment sizes. Collectively, these techniques provided a comprehensive assessment of nanoplastic degradation and enabled an evaluation of the FFPR system's efficacy in reducing polystyrene nanoplastic pollution without producing smaller particles that could elude detection and subsequent removal. The integration

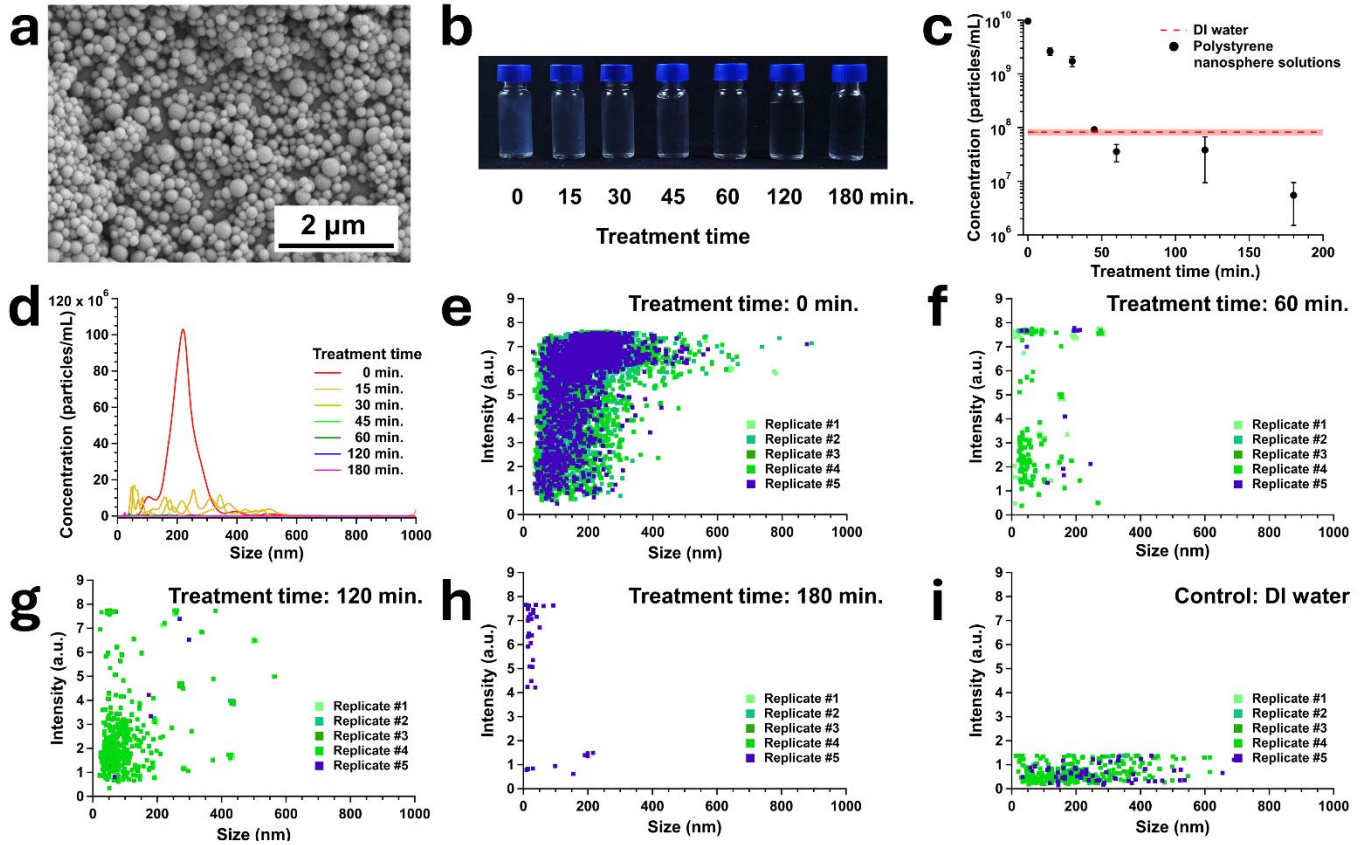

Fig. 2 Plasma-assisted destruction (PAD) of 200-nm polystyrene nanosphere solutions. (a) Scanning electron micrograph of polystyrene nanospheres before plasma treatment. The manufacturer reported size is 208.8±1.4 nm. (b) Photo of plasma-treated 0.001 wt.% polystyrene nanosphere solutions with different treatment times. (c) Plot of total concentrations of polystyrene nanospheres versus treatment time. (d) Plots of concentration of polystyrene nanosphere solutions versus size with different treatment times. (e - h) Plots of particle intensity versus size for polystyrene nanosphere solutions treated for (e) 0 min., (f) 60 min., (g) 120 min., and (h) 180 min., compared to (i) a similar plot for DI water. Note that the first four replicate analyses for the sample with the 180 min. treatment yielded no detectable particles due to its low particle concentration.

of the TOC analysis further elucidated the extent of polymer mineralization to carbon dioxide and offered a crucial understanding for evaluating the environmental safety of the degradation process.

The PAD treatment significantly reduced the particle count of polystyrene nanospheres, as evidenced by a change in the appearance of the solution from turbid to clear, making it indistinguishable from DI water (Figure 2b). The initial concentration of the 0.001% wt. nanoplastic solution measured by NTA was *ca.* 1.22×10^{10} particles per milliliter (Figures 2c and 2d). Note that the mathematical estimation of the particle count in this solution was calculated to be 2.27×10^{9} particles per milliliter. This difference was probably due to the sampling error of small particles and the use of a monomodal distribution function to estimate the particle size by the manufacturer using the dynamic light scattering method. Within the first 60 minutes of the PAD treatment, the FFPR achieved a 98.4% reduction in particle count, lowering this value to approximately 3.56×10^{7} particles per milliliter. By 180 minutes, this reduction reached 99.3%, with the particle count falling to around 5.47×10^{6} particles per milliliter. These concentrations surpassed the ambient particle count in DI water, which stood at about 8.24×10^{7} particles per milliliter. This comparative analysis indicated that the FFPR reduced the particle counts of the nanoplastic solution to below DI water in less than 60 minutes. Importantly, the PAD treatment did not significantly bloat the low particle load in the nanoplastic solution, with the spread of particle size distribution remaining consistent for the first 60 minutes (Figure 2d). Further analysis of the plots of particle intensity versus size (Figures 2e to 2i and Figure S1 in the ESI) was used to quantify the particle identities. Five replicates of particle counts were performed for each sample. As the treatment time increased, the particle intensity values dropped across all sizes of detected nanoparticles. The DI water control featured exclusively particles with intensities less than 2 a.u., which likely represent contaminants inherent to DI water from the water filtration system and other sources (Figure 2i). The particle intensity plots indicate that, by the 180-minute mark, replicates 1st through 4th showed no detectable particulates in the treated solution, confirming the near-complete destruction of particles. Owing to the analytic protocols of the NTA software, recorded NTA video scans that lacked particles were excluded from the final particle analysis. This suggested that actual post-treatment concentrations could be even lower. Note that this study solely focused on the measurable impacts of the FFPR on nanoplastic destruction. Hence, no intensity plots were applied for background correction or data alteration.

This journal is © The Royal Society of Chemistry 2024

Please do not adjust margins

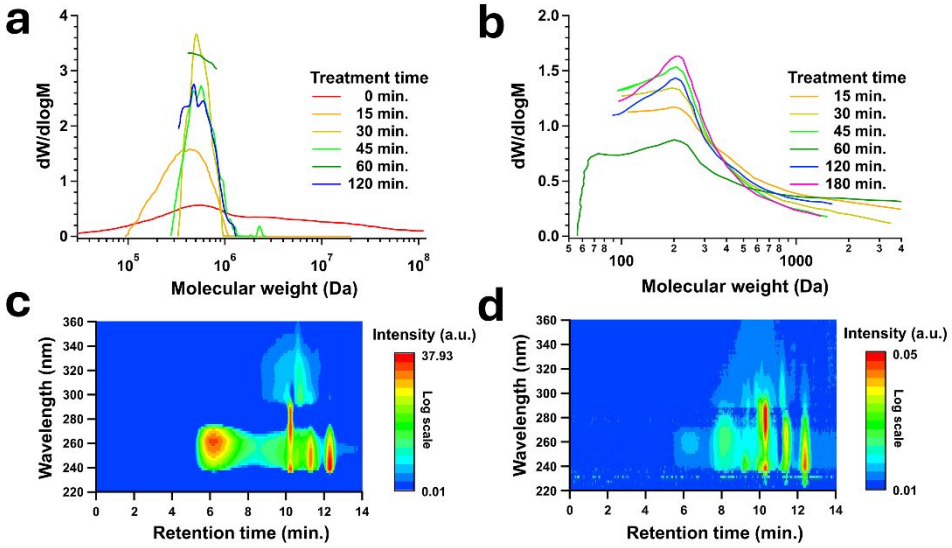

Fig. 3 Size-exclusion chromatography analysis of 200-nm polystyrene nanosphere solutions treated by the plasma-assisted destruction method. Plots of (a) derivative weight fraction of the high mass peak and (b) derivative weight fraction of the low mass peak of polystyrene nanospheres with different treatment times. The low mass peaks appeared after 15 minutes of treatment. No high mass peak was observed after 180 minutes of PAD treatment. Isoabsorbance plots of (c) untreated and (d) 3-hour treated polystyrene nanosphere solutions in stabilized tetrahydrofuran solvent.

The SEC analysis provided further insights into the transformation dynamics of polystyrene nanoplastics during the PAD treatment (Figure 3). A fundamental concern with any nanoplastic degradation method is the potential fragmentation of nanoplastic particles into smaller and potentially more problematic sizes. For this study, the SEC was calibrated using polystyrene latex bead standards for comparative assessments of nanoplastics subjected to various plasma treatments. Initially, the nanoplastic solution demonstrated a broad peak with an average molecular weight of approximately 7.7 MDa (Figure 3a). This broad peak suggested significant variation in polymer chain length among the particles. Within just 15 minutes of PAD treatment, the major SEC peak of the resulting solution became more defined, and its total area decreased, signifying a transition of the degraded nanospheres towards more uniform molecular weights. Additionally, a new secondary peak characterized by an average molecular weight of about 700 Da emerged (Figure 3b). This peak indicated the presence of polystyrene oligomers—short polymer chains that resulted from the breakdown of the original nanospheres. As the PAD treatment progressed, the prominence of the initial major SEC peak diminished and ultimately disappeared by 3 hours while the average mass of the oligomer peak shifted to 298 Da, which approximately corresponds to those of styrene dimers. These results illustrate the FFPR's capability to effectively destroy polystyrene nanospheres into potentially less environmentally impactful molecular components.

The SEC analysis was augmented with a paired UV/Vis absorbance detector, enabling a more comprehensive examination of the sample through an isoabsorbance plot (Figures 3c and 3d). This technique assisted in identifying potential byproducts beyond the primary polystyrene polymers. Initially, the nanoplastic sample exhibited a single sample peak at the 6-minute retention time and three additional peaks between the 10-minute and 12.5-minute retention time. These additional peaks were attributed to the stabilized tetrahydrofuran solvent. After 180 minutes of PAD treatment, the isoabsorbance plot had two distinct peaks between 8 minutes and 10 minutes, alongside a diminished peak corresponding to the original polystyrene nanospheres, signaling significant destruction. However, the chemical identities of these new peaks remain unidentified. These shifts in retention time indicate that these peaks represent compounds distinct from polystyrene which, in turn, signified the formation of new compounds during the degradation process. The inability of SEC to precisely characterize these species highlights the complexity of the reactions and underscores the necessity for further analytical efforts to elucidate their structure and environmental implications. This discovery opens avenues for additional research to fully understand the byproducts of nanoplastic degradation and destruction and to assess their impact on the efficacy and safety of PAD treatments.

3.2 Mineralization and chemical evolution of PS-NPs during plasma treatment

The observed reduction in polystyrene nanoplastic particle count, coupled with the absence of significant populations of smaller particles, necessitated a further investigation into the fate of the degraded plastic materials. To elucidate the underlying degradation mechanisms, the TOC analysis was conducted to serve as a critical metric for quantifying reductions in carbon content indicative of mineralization processes. The sample analysis revealed a decrease in the TOC of the nanoplastic solutions from an initial concentration of 22.3 ppm to 16.2 ppm after three hours of PAD treatment. The initial concentration of carbon was computed from the polystyrene nanoplastics added and the total organic leachate from the

reactor housing and tubing. Thus, without considering the plasma-reduced correction of the leachate, the TOC reduction corresponds to an approximate 27.4% mineralization of the organic content within the PAD treatment period, corroborating the observed decrease in nanoplastic particle count. These findings not only validate the physical destruction of polystyrene nanospheres but also suggest that the PAD method facilitates their transformation through mineralization to form carbon dioxide. This dual effect underscores the FFPR's capability to mitigate nanoplastic pollution not only by reducing the particle count but also by transforming the materials into environmentally benign byproducts. These results contribute to a more comprehensive understanding of the FFPR's environmental impact and its effectiveness in treating nanoplastic pollution.

3.3 Comparison between ozonation treatment and plasma treatment on PS-NPs

The municipal system for the city of Lincoln in Nebraska of the USA employs ozonation treatment for bacterial removal and metal oxidation in potable water.[11] To assess the potential application of the plasma treatment method within such contexts, it is crucial to compare the degradation effects of ozone on polystyrene nanospheres with those by the plasma-assisted method. In contrast to the 0.001 wt.% 200-nm polystyrene nanoplastic solutions treated by the PAD method, the ozone-treated samples exhibited only slight reductions in particle count per milliliter over the same treatment duration while producing a significant number of smaller particle sizes (Figure 4a). The initial solution measured approximately 6.9×10^9 particles per milliliter with a mean size of 175.1 (±61.5) nm. The first 60 minutes of ozonation reduced the particle count to about 5.3×10^9 per milliliter but decreased the average size to 143.4 (±62.8) nm. By the end of the 3-hour treatment period, the particle count had only reduced to about 4.0×10^9 per milliliter. The NTA identified resolvable peaks with mean sizes of 93.0 nm and 230.4 nm, suggesting that not only were the polystyrene particles fragmenting, but the fragments were also beginning to flocculate (Figure 4b). These results indicate that the 3-hour ozonation resulted in a lesser particle reduction compared to even that of the 15-minute plasma-assisted treatment but with a significantly higher density of smaller particles being generated in the process.

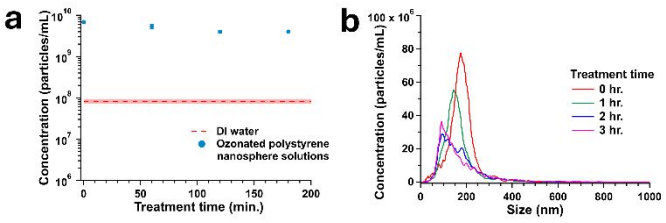

Fig. 4 Ozone-assisted degradation of 200-nm polystyrene nanosphere solutions. (a) Plot of total concentrations of polystyrene nanosphere solutions versus treatment time. (b) Plots of concentrations of polystyrene nanosphere solutions versus size with different treatment times.

4. Discussion

The FFPR system excels in producing a variety of reactive oxygen and nitrogen species; yet the hydroxyl radical, with its optimal balance of oxidative potential and lifespan, plays a central role in the destruction of organic pollutants.[32] Our prior findings indicate that under the current operation and configuration of the FFPR, at least 0.2 mM of hydroxyl radicals per minute are produced in the plasma-assisted treatment method.[33] Consequently, we postulate that hydroxyl radicals act as the primary agents in the plasma-assisted destruction of polystyrene nanospheres. Polystyrene possesses a unique degradation pathway distinct from other common polymers due to its aromatic ring structures.[34] This aromatic component introduces complexities to its degradation mechanism which remains under debate partly due to the potential for multiple concurrent pathways and UV sensitivity.[35]

We proposed a mechanism for the cyclic degradation of polystyrene using hydroxyl radicals generated in the plasma, akin to mechanisms observed in UV degradation processes (Figure 5). The degradation cycle likely initiates with hydrogen abstraction by hydroxyl radicals to form carbon-centered macroradicals (Figure 5 Step A). These radicals subsequently interact with oxygen to form hydroperoxyl radicals, which can further propagate the reaction by abstracting hydrogen atoms from other polymer chains (Figure 5 Step B). The resultant structures undergo photolysis-like reactions to yield alkoxyl macroradicals and hydroxyl radicals, both of which can further propagate the reaction. The alkoxyl structures are expected to undergo β-scission through the Norrish-Yang reaction,[36] producing new, shorter polymers capped by alkenes or enols (Figure 5 Step C). These are primed to participate once again in the initial hydrogen abstraction, perpetuating the degradation cycle (Figure 5 Step A). Alternatively, the radicalized shortened polystyrene may react with another similarly radicalized polymer or hydroxyl radicals to yield new crosslinked products (Figure 5 Step D1). These interactions might theoretically lead to an increase in smaller particles. Contrary to this possibility, as the plasma-assisted treatment time increased, our experimental results predominantly indicated the formation of short oligomers, especially dimers, rather than a proliferation of smaller particles and fragments. Our observed formation of oligomers and the specific reductions in particle size and TOC under plasma-assisted conditions lend further insights into these mechanisms, suggesting a degradation pathway analogous to photolysis. The emergence of two new peaks in the isoabsorbance plots could be attributed to the creation of polyenes or ketone structures in terminal alkenes resulting from the degradation of polystyrene. These shorter oligomers are expected to undergo further mineralization via hydroxyl radical attacks and oxidation (Figure 5 Step D2). The convergence of these results indicates that the plasma-assisted treatment degrades the polystyrene nanoplastics through a cyclic radicalization like photolysis, facilitating greater efficiencies compared to other non-radical degradation methods. In contrast, results from the ozonated polystyrene nanosphere solution show an increase in smaller particles, highlighting the

This journal is © The Royal Society of Chemistry 2024

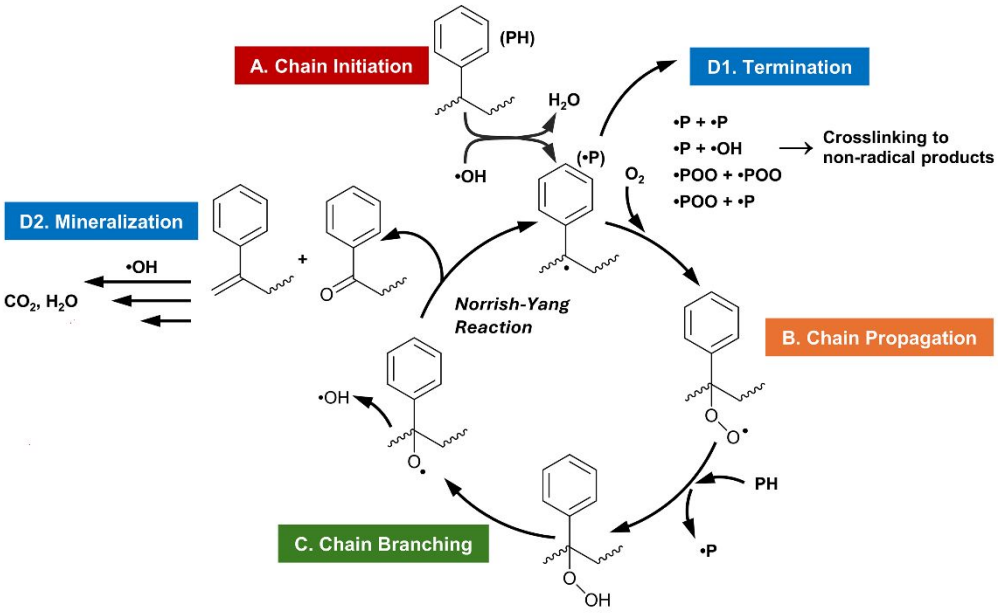

Fig. 5 Proposed cyclic mechanism for the autoxidation of polystyrene nanospheres driven by hydroxyl radicals.

limitations of ozonation which, despite being an advanced oxidation method, lacks the oxidating power to initiate a full cyclic radical decay as in our proposed plasma-assisted mechanism.

Unlike many water treatment methods that rely on consumables such as filters or disposable electrodes, the plasma-assisted destruction (PAD) methodology primarily utilizes an inducer gas and electricity to remove nanoplastic particles. Although the efficiency under ambient conditions is slightly lower for our demonstrated PAD method, the primary input for our FFPR reactor is electricity. Our FFPR reactor was demonstrated to have a notable efficiency with a power consumption of approximately 35 W.[29] This measurement was obtained by either averaging the product of temporal applied voltage and current over time or determining the area of the "elliptical" Lissajous plot of charge versus applied voltage (See Figure S2 in the ESI).[37] Our estimation of this power value is consistent and aligns with findings from other studies employing similar FFPR systems, showcasing its stable energy requirements for plasma generation. In the city of Lincoln, Nebraska where the average electricity cost for homes is 10.22 cents per kWh in 2024,[38] the operational cost for a 3-hour treatment cycle for our illustrated polystyrene nanoplastic solution amounted to merely 1.07 cents or 27 cents/hr./gal. Compared to the ozone generator, which has a power consumption of approximately 115 W or 88.7 cents/hr./gal. This economic analysis, coupled with the reactor's demonstrated efficacy in degrading polystyrene nanoplastics, underscores the potential for the widespread application of the PAD methodology. Efficiency can further be increased by refining certain variables such as substituting ambient air with a pure oxygen atmosphere as the plasma inducer, which has been shown to amplify oxidative degradation and eliminate side products such as nitrates in similar studies through increased production of reactive oxygen species.[35]

The interdisciplinary nature of this research bridges the gap between nanoscience, environmental science, and applied chemistry, highlighting its broad applicability and relevance. The integration of plasma physics with chemical engineering in our reactor design not only enhances the understanding of reactive species interactions with nanoplastics but also paves the way for innovations in chemical synthesis and waste management. The plasma-assisted destruction methodology explored in this study demonstrates superior efficiency in both time and particle removal rates through its near-complete chemical breakdown of nanoplastic contaminants. While all treatment methods for microplastics and nanoplastics offer opportunities for enhancement, many conventional approaches like industrial filtration face challenges such as the generation of contaminated filter media. Although current lab-scale plasma reactors do not generate contaminated media, they cannot meet the throughput of industrial-scale filtration systems. To close the gap in throughput capabilities, future research should focus on optimizing reactor designs, operational parameters, and plasma inducers to enhance the processing rates without compromising efficiency or environmental safety. This engineering challenge can potentially achieve scalability through various pathways such as optimizing the reactor geometries, residence time, and even optimizing the circuit itself. Furthermore, the potential and complementary applications of this methodology can be extended into public health where effective water purification methods are crucial for removing toxic organic substances and preventing their entry into the human body. By linking the degradation mechanisms of polystyrene nanoplastics to their environmental and health impacts, our study contributes to the

development of safer, more effective strategies for managing nanoplastic pollution.

5. Conclusions

This study successfully demonstrated the efficacy of the plasma-assisted destruction (PAD) methodology with a falling-film plasma reactor (FFPR) in destroying polystyrene nanoplastics within aqueous solutions. Experimental trials with solutions containing 0.001 wt.% polystyrene nanoparticle solids (approximately 2×10^{10} particles/mL or 100 ppm) achieved a destruction removal efficiency (DRE) of 98.4% by particle count within one hour of PAD treatment and 99.3% after three hours of treatment. In the major pathway of our hypothesized reaction mechanism, hydroxyl radicals generated by the plasma treatment abstract hydrogen atoms from the polystyrene chains to initiate carbon-centered macroradicals on the tertiary carbons. This reaction is expected to be followed by β-scission, facilitating a cyclic breakdown of the nanoplastic particles. Alternatively, in a minor pathway, the incoming radicals could directly interact with the polymer chain to form acetophenone without generating additional radicals. Both hypothesized pathways are posited to culminate in the mineralization of the polymer, yielding carbon dioxide and water as end products. The demonstrated destruction efficacy of the FFPR illustrates its potential applicability to a broad range of carbon chain polymers including commonly used polyolefins such as polyethylene and polypropylene. For the next stage of PAD developments, future research should focus on operando structure characterization and quantification of byproducts, especially in complex solutions featuring mixed-size compositions. Such studies will enhance our understanding of the plastic degradation mechanisms and enable pragmatic evaluations of the efficacy and versatility of this method for broader practical and complementary applications.

Author contributions

Winburn: Conceptualization (equal); Writing – original draft (equal); Writing – review and editing (supporting); formal analysis (equal); Visualization (equal); Validation (equal); Methodology (equal); Investigation (equal). **Alvarado**: Investigation (equal); Validation (equal); Writing – review and editing (supporting). **Cheung**: Conceptualization (equal); Writing – original draft (equal); Writing – review and editing (lead); Formal Analysis (equal); Visualization (equal); Supervision (lead); Resources (lead); Project Administration (lead); Funding Acquisition (lead).

Conflicts of interest

There are no conflicts to declare.

Data Availability

The data supporting this article have been included as part of the Supplementary Information.

Acknowledgments

This project was in part funded by the Department of Chemistry at the University of Nebraska-Lincoln. The NTA experiment was performed using the facility in The Biomedical and Obesity Research Core (BORC) of the Nebraska Center for Prevention of Obesity Diseases (NPOD). The BORC receives support from the NIH (NIGMS) COBRE IDeA award (NIH P20GM104320). The NTA experiments were repeated in the Nebraska Nanoscale Facility: National Nanotechnology Coordinated Infrastructure and the Nebraska Center for Materials and Nanoscience, which are supported by the NSF under Award ECCS: 2025298, and the Nebraska Research Initiative. Additionally, we would like to thank Dustin Peterson and the UNL Biological Process Development Facility for their assistance in running the TOC and the valuable discussion. The contents of this publication are the sole responsibility of the authors and do not necessarily represent the official views of the NIH or NIGMS.

Notes and references

1. R. Geyer, J. R. Jambeck, and K. L. Law, *Science Advances*, 2017, **3**, e1700782.
2. A. Chamas, H. Moon, J. Zheng, Y. Qiu, T. Tabassum, J. H. Jang, M. Abu-Omar, S. L. Scott, and S. Suh, *ACS Sustainable Chemistry & Engineering*, 2020, **8**, 3494.
3. J. A. I. do Sul, and M. F. Costa, *Environmental Pollution*, 2014, **185**, 352.
4. S. Kihara, I. Köper, J. P. Mata, and D. J. McGillivray, *Advances in Colloid and Interface Science*, 2021, **288**, 102337.
5. A. A. Koelmans, E. Besseling, and W. J. Shim, in *Marine Anthropogenic Litter*, eds. M. Bergmann, L. Gutow, and M. Klages, Springer, New York, 2015, pp. 325.
6. L. A. Amaral-Zettler, E. R. Zettler, and T. J. Mincer, *Nature Reviews Microbiology*, 2020, **18**, 139.
7. R. Lehner, C. Weder, A. Petri-Fink, and B. Rothen-Rutishauser, *Environmental Science & Technology*, 2019, **53**, 1748.
8. L. Rubio, R. Marcos, and A. Hernández, *Journal of Toxicology and Environmental Health, Part B*, 2020, **23**, 51.
9. G. M. Zarus, C. Muianga, C. M. Hunter, and R. S. Pappas, *Science of the Total Environment*, 2021, **756**, 144010.
10. M. L. Sikosana, K. Sikhwivhilu, R. Moutloali, and D. M. Madyira, *Procedia Manufacturing*, 2019, **35**, 1018.
11. Lincoln Water Systems, 2023 Annual Drinking Water Quality Report, https://www.lincoln.ne.gov/City/Departments/LTU/Utilities/LWS).
12. X. Zhang, Y. Zhai, Z. Wang, X. Liu, X. Liu, Y. Zhou, G. Liu, and M. Xu, *Separation and Purification Technology*, 2023, **322**, 124245.
13. W. Li, C. Wu, Z. Xiong, C. Liang, Z. Li, B. Liu, Q. Cao, J. Wang, J. Tang, and D. Li, *Science Advances*, 2022, **8**, eade1731.
14. M. Urso, M. Ussia, and M. Pumera, *Nature Reviews Bioengineering*, 2023, **1**, 236.
15. J. Lu, R. Hou, Y. Wang, L. Zhou, and Y. Yuan, *Water Research*, 2022, **226**, 119277.
16. J. E. Foster, *Physics of Plasmas*, 2017, **24**, 055501.
17. G. R. Stratton, C. L. Bellona, F. Dai, T. M. Holsen, and S. M. Thagard, *Chemical Engineering Journal*, 2015, **273**, 543.

 This journal is © The Royal Society of Chemistry 2024

18. Y. Yang, Y. I. Cho, and A. Fridman, *Plasma Discharge in Liquid: Water Treatment and Applications*, CRC Press, Boca Raton, 2012.
19. H. Conrads, and M. Schmidt, *Plasma Sources Science and Technology*, 2000, **9**, 441.
20. E. Gomez, D. A. Rani, C. Cheeseman, D. Deegan, M. Wise, and A. Boccaccini, *Journal of Hazardous Materials*, 2009, **161**, 614.
21. D. B. Miklos, C. Remy, M. Jekel, K. G. Linden, J. E. Drewes, and U. Hübner, *Water Research*, 2018, **139**, 118.
22. V. Scholtz, J. Pazlarova, H. Souskova, J. Khun, and J. Julak, *Biotechnology Advances*, 2015, **33**, 1108.
23. M. Moreau, N. Orange, and M. Feuilloley, *Biotechnology Advances*, 2008, **26**, 610.
24. Y. Gorbanev, D. O'Connell, and V. Chechik, *Chemistry–A European Journal*, 2016, **22**, 3496.
25. A. Rida Galaly, G. Van Oost, and N. Dawood, *ACS Omega*, 2024, **9**, 21174.
26. B. Tabu, K. Akers, P. Yu, M. Baghirzade, E. Brack, C. Drew, J. H. Mack, H.-W. Wong, and J. P. Trelles, *International Journal of Hydrogen Energy*, 2022, **47**, 39743.
27. H. M. Nguyen, and M. L. Carreon, *ACS Sustainable Chemistry & Engineering*, 2022, **10**, 9480.
28. H. Radhakrishnan, S. Gnangbe, A. Duereh, S. U. I. Uday, A. Lusi, H. Hu, H. Hu, M. M. Wright, and X. Bai, *Green Chemistry*, 2024, **26**, 9156.
29. M. A. Malik, *Plasma Chemistry and Plasma Processing*, 2010, **30**, 21.
30. B. Wang, M. Xu, C. Chi, C. Wang, and D. Meng, *Journal of Advanced Oxidation Technologies*, 2017, **20**, 20170021.
31. J. Wang, X. Zhao, A. Wu, Z. Tang, L. Niu, F. Wu, F. Wang, T. Zhao, and Z. Fu, *Environmental Pollution*, 2021, **268**, 114240.
32. J. L. Wang, and L. J. Xu, *Critical Reviews in Environmental Science and Technology*, 2012, **42**, 251.
33. M. R. Winburn, E. L. De Leon, K. L. Schuelke, W.-N. Mei, H. Li, and C. L. Cheung, *Chemical Engineering Journal*, 2024, **486**, 150237.
34. E. Yousif, and R. Haddad, *SpringerPlus*, 2013, **2**, 1.
35. J. F. Rabek, and B. Rånby, *Journal of Polymer Science: Polymer Chemistry Edition*, 1974, **12**, 273.
36. S. E. Braslavsky, *Pure and Applied Chemistry*, 2007, **79**, 293.
37. P. Floran, and B. Tom, in *Atmospheric Pressure Plasma*, eds. N. Anton, and C. Zhiqiang, IntechOpen, Rijeka, 2018, DOI: 10.5772/intechopen.80433, p. Ch. 2.
38. Lincoln Electric Systems, Lincoln Electric System Winter 2024 Regional Utility Bill Comparison, https://www.les.com/rates/residential-rates, (accessed on 6/11/2024).

Data Availability Statement

The data supporting this article have been included as part of the Electronic Supplementary Information.